

# A Carbon–Air Battery for High Power Generation\*\*

Binbin Yang, Ran Ran,\* Yijun Zhong, Chao Su, Moses O. Tadé, and Zongping Shao\*

**Abstract:** We report a carbon–air battery for power generation based on a solid-oxide fuel cell (SOFC) integrated with a ceramic  $\text{CO}_2$ -permeable membrane. An anode-supported tubular SOFC functioned as a carbon fuel container as well as an electrochemical device for power generation, while a high-temperature  $\text{CO}_2$ -permeable membrane composed of a  $\text{CO}_3^{2-}$  mixture and an  $\text{O}^{2-}$  conducting phase ( $\text{Sm}_{0.2}\text{Ce}_{0.8}\text{O}_{1.9}$ ) was integrated for in situ separation of  $\text{CO}_2$  (electrochemical product) from the anode chamber, delivering high fuel-utilization efficiency. After modifying the carbon fuel with a reverse Boudouard reaction catalyst to promote the in situ gasification of carbon to  $\text{CO}$ , an attractive peak power density of  $279.3 \text{ mW cm}^{-2}$  was achieved for the battery at  $850^\circ\text{C}$ , and a small stack composed of two batteries can be operated continuously for 200 min. This work provides a novel type of electrochemical energy device that has a wide range of application potentials.

The rapidly expanding energy demand, worsening environmental pollution, and increasing concentration of  $\text{CO}_2$  in the atmosphere from the inefficient utilization of fossil fuels have resulted in extensive research activities to search for new energy sources and alternative means of utilizing available energy resources more efficiently and with less environmental impact. The energy level requirements for different fields of application can vary significantly, from megawatts for stationary power applications, to kilowatts for domestic usage, and microwatts for consumer electronics applications. In particular, there is a rapidly growing demand for portable power sources. Furthermore, the energy-density requirement for portable power sources has been continuously increasing and thus new technologies that can lead to higher energy densities are highly desired.

Carbon is one of the most important elements on earth, and carbon resources are abundant and readily available. Coal, coke, graphite, municipal solid waste, natural gas, and other carbonaceous materials including biomass are all potential sources of carbon. The efficient use of carbon as an energy material may realize both a sustainable power supply and reduced greenhouse-gas emissions. Carbon has been widely applied as an energy material in lithium-ion batteries (LIBs),<sup>[1]</sup> where it functions as a lithium-ion insertion host instead of as a real fuel, and exhibits a theoretical capacity of  $372 \text{ mAh g}^{-1}$  (graphite).<sup>[2]</sup> However, the energy density of these LIBs is not sufficient for many portable applications. Converting carbon into  $\text{CO}_2$  releases a very high energy density ( $20 \text{ kWh L}^{-1}$ ), compared to other fuels such as  $\text{H}_2$  ( $2.4 \text{ kWh L}^{-1}$ ),  $\text{CH}_4$  ( $4.2 \text{ kWh L}^{-1}$ ), and diesel ( $9.8 \text{ kWh L}^{-1}$ ), thus making carbon highly attractive for portable applications.<sup>[3]</sup> Carbon is a solid substance and can thus be stored and transported more conveniently and safely than gaseous and liquid fuels, and does not require a radical change to the current infrastructure.

Conventional power generation from carbon (coal) uses combustion technology,<sup>[4]</sup> which has a low energy-conversion efficiency because of the limitations of the Carnot cycle. Fuel cells have recently received considerable attention as clean alternatives for electricity generation, where chemical energy is converted into electric power electrochemically with high efficiency and low emissions.<sup>[5]</sup> Carbon can be used as a fuel in a special type of fuel cell known as a direct carbon fuel cell (DCFC),<sup>[6]</sup> where an ultrahigh efficiency of 100% could be realized. However, for the DCFCs that use hydroxide or molten carbonate as the electrolyte, the carbon must have a sufficiently high electrical conductivity because it also functions as a current collector.<sup>[6a,b]</sup> The hydroxide electrolyte is unfortunately easily contaminated by  $\text{CO}_2$ , resulting in carbonate formation in the carbon fuel, which can rapidly deactivate the fuel-cell performance.<sup>[3b]</sup> DCFCs that use a carbonate electrolyte exhibit greatly enhanced electrolyte stability, but  $\text{CO}_2$  is consumed at the cathode,<sup>[7]</sup> therefore  $\text{CO}_2$  is required to circulate between the two electrodes, which results in a complex fuel-cell system. Corrosion of carbonate and hydroxide is also a serious problem for the operational stability of DCFCs that use these electrolytes. The application of solid oxide as the electrolyte of DCFCs can solve the problem of corrosion, but the small carbon–electrode–electrolyte triple phase boundary (TPB) often results in a poor power output. As a result, although significant progress has been made on DCFCs over the past decades, they are not suitable for portable applications because of the complexity of the system, the poor power density, the low energy density (because of the small amount of carbon at the anode), or the poor operational stability.<sup>[8]</sup>

[\*] B. B. Yang, Prof. R. Ran, Y. J. Zhong, Prof. Z. P. Shao  
State Key Laboratory of Materials-Oriented Chemical Engineering  
College of Chemistry & Chemical Engineering  
Nanjing Tech University  
5 Xin Mofan Road, Nanjing 210009 (P.R. China)  
E-mail: shaozp@njtech.edu.cn

Dr. C. Su, Prof. M. O. Tadé, Prof. Z. P. Shao  
Department of Chemical Engineering, Curtin University  
Perth, Western Australia 6845 (Australia)

[\*\*] This work was supported by the Key Projects in Nature Science Foundation of Jiangsu Province under contract no. BK2011030, the National Science Foundation for Distinguished Young Scholars of China under contract no. 51025209 and the Priority Academic Program Development of Jiangsu Higher Education Institutions. We acknowledge an ARC Future Fellowship under contract FT100100134.

Supporting information for this article is available on the WWW under <http://dx.doi.org/10.1002/anie.201411039>.

As gas diffusion is much easier than solid diffusion, one way to greatly increase the electrode reaction rate using a carbon fuel is to first convert carbon to CO in a reverse Boudouard reaction ( $C + CO_2 \rightarrow 2CO$ ); CO is then directly utilized as the fuel for solid-oxide fuel cells (SOFCs).<sup>[9]</sup> However, CO is difficult to separate from the higher oxidation product  $CO_2$  in conventional fuel cells, thus reducing the fuel utilization and consequently, the overall system efficiency. Integrating a conventional  $CO_2/CO$  separation unit into fuel cells can substantially increase the volume and the complexity of the system, which is unfavorable for portable applications.

Herein, we report an electrochemical device, known as a carbon–air battery, consisting of a tubular SOFC integrated with a carbonate-doped ceria composite membrane for in situ  $CO/CO_2$  separation, as a portable power source with high power output and energy density. The carbon fuel was modified with a catalyst to promote the reverse Boudouard reaction and allow the gasification of carbon to CO by reacting with the in situ electrochemical oxidation product  $CO_2$  in the anode chamber; CO served as the fuel and effectively increased the TPB and thus the power density. The membrane separated  $CO_2$  from CO and released it to the surrounding environment, thus allowing a high CO partial pressure in the anode chamber.

As shown in Figure 1 a,b, the tubular SOFC is not only an electrochemical device for electricity generation, but also a fuel container. To realize a high power output, the tubular cell should have a high activity for the electrocatalytic oxidation of CO, and the electrolyte should be highly densified to avoid the direct mixing of fuel gas and oxidant. Figure 1c shows the surface morphology of the prepared yttria-stabilized zirconia (YSZ) electrolyte, which was sintered and composed of grains that were mostly 3–5  $\mu m$  in size. No obvious surface defects were observed, which can be attributed to the good sinterability of YSZ and the large shrinkage of the tubular anode substrate during the sintering

process. The cross-sectional view of the complete cell with a  $La_{0.8}Sr_{0.2}MnO_3$  (LSM)-YSZ cathode is shown in Figure 1d. The YSZ electrolyte layer was homogeneous in thickness (ca. 13  $\mu m$ ) and well-sintered with few enclosed holes. Excellent adhesion of the electrolyte layer to the anode substrate was observed. The reduced anode substrate was highly porous, ensuring the free diffusion of CO fuel to the TPB. High open-circuit voltages (OCVs) in the range 1.1–1.15 V and almost linear response of cell voltage to polarization current were obtained for the cell operating on  $H_2$  fuel (Figure S1 in the Supporting Information), further demonstrating good cell efficiency.

In situ separation of  $CO_2$  and CO is critically important for increasing the fuel utilization efficiency. Recently, a mixed  $CO_3^{2-}$  and  $O^{2-}$  conducting membrane was developed for high-temperature  $CO_2$  separation with a  $CO_2$  permeation selectivity of 100%.<sup>[10]</sup> A schematic diagram of the working principle is shown in Figure S2 (see the Supporting Information). The  $O^{2-}$  conducting phase has been demonstrated to play a more critical role in  $CO_2$  permeation than the  $CO_3^{2-}$  conducting phase because the  $O^{2-}$  conductivity of oxide is typically much lower than  $CO_3^{2-}$  conductivity of molten carbonate.<sup>[10]</sup> Therefore, a  $Sm_{0.2}Ce_{0.8}O_{1.9}$  (SDC) material that possesses a high ionic conductivity was selected as the  $O^{2-}$  conducting phase in this study. The membranes prepared by a conventional infiltration method were not well-densified because of the poor wettability of  $O^{2-}$ -conducting ceramic by carbonate.<sup>[11]</sup> To increase the wetting of the SDC surface, a SDC membrane with an appropriate amount of carbonate ( $Li_2CO_3$ ,  $Na_2CO_3$ , and  $K_2CO_3$ ) was presintered; most of the carbonate was lost during the sintering because of the high fluidity of carbonate at the high temperature (520 °C) of the sintering process, as shown in Figure 2a. The scaffold is a porous structure comprising piled spherical particles with a homogeneous size of 1–1.5  $\mu m$ . These SDC particles were fused to provide  $O^{2-}$  conducting paths, thus minimizing the  $O^{2-}$  diffusion polarization resistance, which is critical for achieving a high  $CO_2$  flux. After the infiltration, the void space between the SDC particles was completely filled with carbonate to form a densified SDC–carbonate dual-phase membrane (Figure 2b). This behavior indicates that the capillary force was strong enough to drive the molten carbonate throughout the whole membrane. According to related energy dispersive X-ray (EDX) analysis results (Figure S3), the content of molten carbonate was calculated to be approximately 10–15 wt. % based on the amount of Na and K

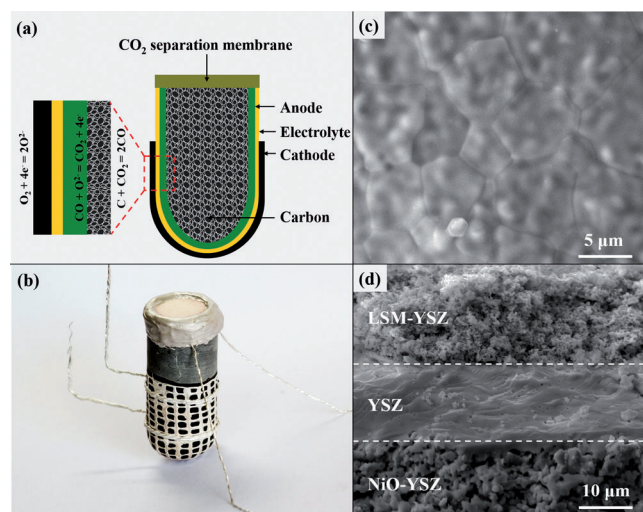


**Figure 1.** a) Diagram and b) photograph of the carbon–air battery. SEM images of c) surface morphology of the YSZ electrolyte, and d) the cross-sectional view of the tubular SOFC with the LSM-YSZ cathode.

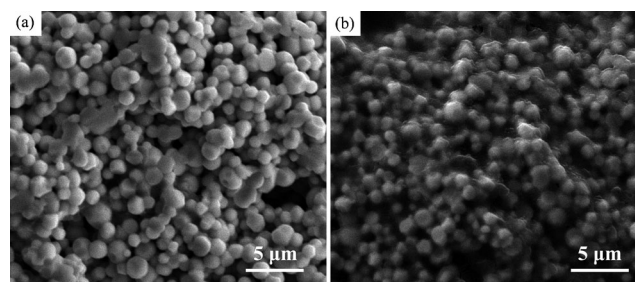


**Figure 2.** SEM images of a) the porous SDC scaffold and b) the SDC–carbonate dual-phase membrane.

(Li cannot be detected by EDX because of its small atomic weight), further confirming that the SDC phase was filled with molten carbonate.

Excellent gas-tightness of the membrane was demonstrated by the permeation test because no helium (a probe gas) was detected at the sweep side atmosphere. This result implies a lack of connecting pinholes in the as-fabricated membrane. The temperature dependence of the CO<sub>2</sub> permeation flux through the dual phase membrane is shown in Figure 3. A sharp increase of permeation flux from 0.11

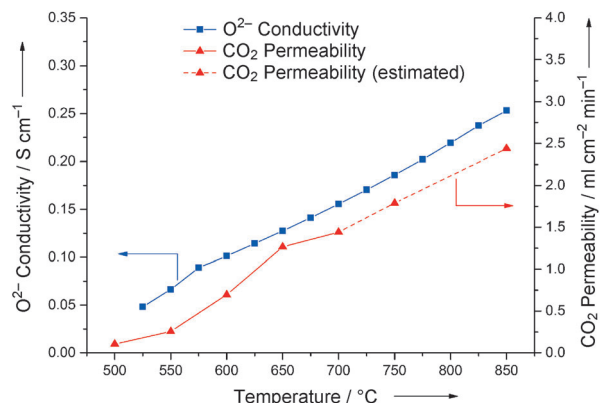


**Figure 3.** Temperature dependence of CO<sub>2</sub> permeation flux through the dual-phase membrane and the total O<sub>2</sub><sup>2-</sup> conductivity of SDC.

(500 °C) to 1.50 mL min<sup>-1</sup> cm<sup>-2</sup> (700 °C) was observed, and arose mainly from the increase in O<sub>2</sub><sup>2-</sup> conductivity of the SDC. The observed permeation fluxes were much higher than the values reported for similar membranes.<sup>[11a]</sup> Such an improvement is likely due to the much improved densification of the membrane fabricated by using the technique reported here. The permeation flux above 700 °C was not obtained because carbonate melts easily at higher temperatures. Assuming the permeation flux is solely determined by the O<sub>2</sub><sup>2-</sup> conductivity, the CO<sub>2</sub> permeation fluxes at higher temperatures can be estimated from the total conductivity of the SDC (Figure 3). The CO<sub>2</sub> flux can increase to 1.79 mL min<sup>-1</sup> cm<sup>-2</sup> at 750 °C, and further to 2.44 mL min<sup>-1</sup> cm<sup>-2</sup> at 850 °C.

In these carbon–air batteries, the carbon acted as an energy carrier, while the produced CO was used directly as the fuel for electric power generation. The CO formation rate was closely related to properties of the carbon (such as structure, surface defects, surface functional groups, and specific surface areas), the catalyst, and the operation temperature. The Fe<sub>m</sub>O<sub>n</sub>-M<sub>x</sub>O (M = Li, K, Ca) catalyst, which demonstrated a high activity for the reverse Boudouard reaction,<sup>[9b]</sup> was used to modify the carbon fuels. In this work, four types of carbon with different specific surface areas were investigated. As shown in Figure S4, a rougher carbon-catalyst surface was observed for a carbon fuel with a higher specific surface area, indicative of the creation of a larger contacting area between the catalyst and the carbon fuel, which could benefit the reverse Boudouard reaction. The carbon–air battery was thus tested using activated carbon

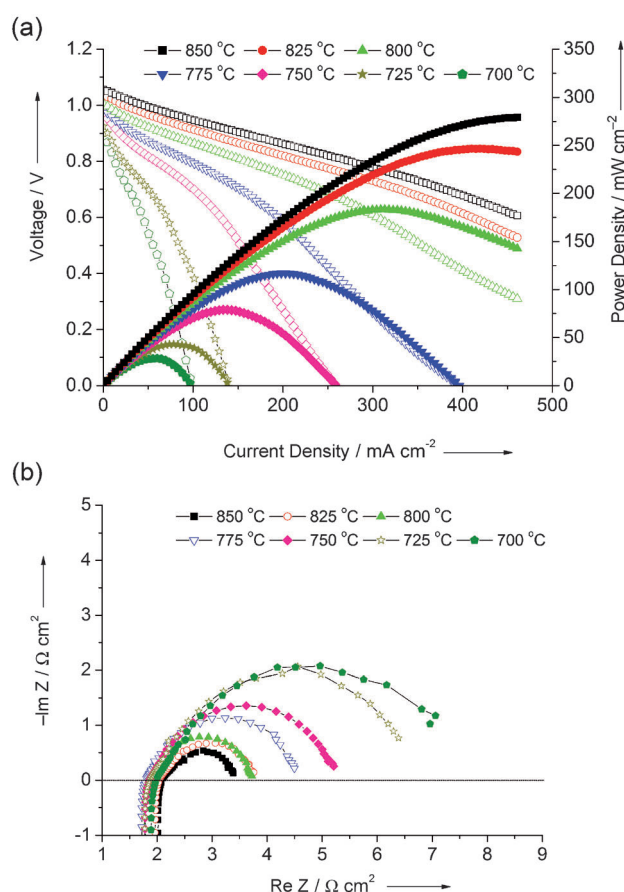


**Figure 4.** a) *I*–*V* and *I*–*P* curves and b) impedance spectra of the carbon–air battery operating with activated carbon (a specific surface area of 1825 m<sup>2</sup> g<sup>-1</sup>) at various temperatures.

with a high specific surface area (1825 m<sup>2</sup> g<sup>-1</sup>) as the fuel, loading with the Fe<sub>m</sub>O<sub>n</sub>-M<sub>x</sub>O catalyst. As shown in Figure 4a, an OCV of 1.056 V and a peak power density (PPD) of 279.3 mW cm<sup>-2</sup> at 850 °C was reached, thus suggesting the practical applicability for this carbon–air battery. The corresponding electrochemical impedance spectroscopy (EIS) results are presented in Figure 4b. The intercepts of the impedance curve with the axis in the high-frequency region was considered as the ohmic resistance (*R*<sub>Ω</sub>), while the intercepts in the low-frequency region was considered as the total resistance, which included *R*<sub>Ω</sub>, the concentration polarization resistance (*R*<sub>pl</sub>), and the effective interfacial polarization resistance (*R*<sub>p2</sub>).<sup>[12]</sup> The *R*<sub>Ω</sub> value was almost unchanged while the *R*<sub>p</sub> value increased with the reduction of operation temperature. The rate of the reverse Boudouard reaction decreased at lower temperature and led to a lower CO concentration within the anode chamber; the electrocatalytic oxidation rate of CO also decreased. Both factors contributed to the increase of the *R*<sub>p</sub> value. The effect of the carbon source on the power output of the carbon–air battery was also examined with the results presented in Figure S5. The increase in the specific surface area of the carbon resulted in increased PPDs. This observation suggests that the cell power output is strongly limited by the reverse Boudouard reaction rate, which is closely related to the operation



temperature, the specific surface area of the carbon, and the contact area between the catalyst and the carbon fuel.

The relatively low voltage of the single carbon–air battery means that stacking is necessary to achieve sufficient power density and voltage for practical applications. A small stack composed of two batteries in series with  $\text{Ba}_{0.95}\text{La}_{0.05}\text{FeO}_{3-\delta}$  (BLF) cathodes was tested (the morphology and performance of cell is shown in Figure S6). The OCV of the stack reached 2.12 V at 825 °C. When the stack was discharged at a constant polarization current of 300 mA, the stack voltage was stable over the initial 120 min, and then the stack could be operated continuously for another 80 min. (Figure 5). Approximately

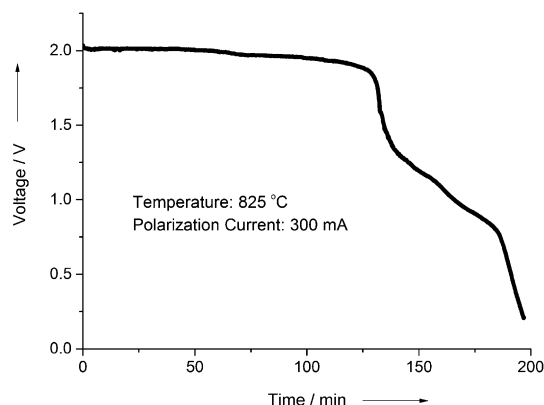


**Figure 5.** Stack voltage as a function of time at 825 °C under a constant polarization current of 300 mA.

3600 coulombs of charge were released during the whole test, which was equivalent to the amount of electricity generated by 0.224 g carbon through an electrochemical reaction. This result means that only 14.36% of the total carbon fuel was converted to electricity. Upon disassembling the cell, it was found that there was still a considerable amount of unreacted carbon in an agglomerated state in the anode chamber of the tubular SOFC; clearly the catalyst became deactivated after the continuous operation. Hence, the development of a more stable and active catalyst for carbon gasification is of critical importance to allow the carbon–air battery to continuously discharge for a longer time.

In summary, a carbon–air battery based on a tubular SOFC integrated with a ceramic membrane for in situ  $\text{CO}/\text{CO}_2$  separation was successfully developed and provides high energy density and fuel utilization efficiency. A peak

power density of  $279.3 \text{ mWcm}^{-2}$  was achieved at 850 °C for a single battery. A small stack composed of two batteries was also built and tested, and delivered continuous operation for 200 min. This system is thus highly attractive for portable power applications. Further efforts will be made toward the development of catalysts to increase the carbon gasification rate and improving the long-term stability of the batteries for practical applications.

Received: November 13, 2014

Published online: January 23, 2015

**Keywords:** carbon–air batteries · fuel cells · gas diffusion · homogeneous catalysis · separation membranes

- [1] M. Winter, R. J. Brodd, *Chem. Rev.* **2004**, *104*, 4245–4270.
- [2] H. Li, Z. Wang, L. Chen, X. Huang, *Adv. Mater.* **2009**, *21*, 4593–4607.
- [3] a) C. R. Jiang, J. J. Ma, A. D. Bonaccorso, J. T. S. Irvine, *Energy Environ. Sci.* **2012**, *5*, 6973–6980; b) S. Zecevic, E. M. Patton, P. Parhami, *Carbon* **2004**, *42*, 1983–1993.
- [4] B. Buhre, L. Elliott, C. Sheng, R. Gupta, T. Wall, *Prog. Energy Combust. Sci.* **2005**, *31*, 283–307.
- [5] Z. Shao, C. Zhang, W. Wang, C. Su, W. Zhou, Z. Zhu, H. J. Park, C. Kwak, *Angew. Chem. Int. Ed.* **2011**, *50*, 1792–1797; *Angew. Chem.* **2011**, *123*, 1832–1837.
- [6] a) L. Guo, J. M. Calo, E. DiCocco, E. J. Bain, *Energy Fuels* **2013**, *27*, 1712–1719; b) L. Kouchachvili, M. Ikura, *Int. J. Hydrogen Energy* **2011**, *36*, 10263–10268; c) A. Elleuch, J. Yu, A. Boussetta, K. Halouani, Y. Li, *Int. J. Hydrogen Energy* **2013**, *38*, 8514–8523; d) B. Cantero-Tubilla, C. Xu, J. W. Zondlo, K. Sabolsky, E. M. Sabolsky, *J. Power Sources* **2013**, *238*, 227–235; e) R. Liu, C. Zhao, J. Li, F. Zeng, S. Wang, T. Wen, Z. Wen, *J. Power Sources* **2010**, *195*, 480–482; f) J. Zhou, X. Ye, L. Shao, X. Zhang, J. Qian, S. Wang, *Electrochim. Acta* **2012**, *74*, 267–270; g) W. A. McPhee, M. Boucher, J. Stuart, R. S. Parnas, M. Koslowski, T. Tao, B. A. Wilhite, *Energy Fuels* **2009**, *23*, 5036–5041.
- [7] S. Giddey, S. Badwal, A. Kulkarni, C. Munnings, *Prog. Energy Combust. Sci.* **2012**, *38*, 360–399.
- [8] T. M. Guer, *Chem. Rev.* **2013**, *113*, 6179–6206.
- [9] a) Y. Nabae, K. D. Pointon, J. T. Irvine, *Energy Environ. Sci.* **2008**, *1*, 148–155; b) Y. Wu, C. Su, C. Zhang, R. Ran, Z. Shao, *Electrochem. Commun.* **2009**, *11*, 1265–1268.
- [10] M. Anderson, Y. Lin, *J. Membr. Sci.* **2010**, *357*, 122–129.
- [11] a) J. L. Wade, C. Lee, A. C. West, K. S. Lackner, *J. Membr. Sci.* **2011**, *369*, 20–29; b) Z. Rui, M. Anderson, Y. Li, Y. Lin, *J. Membr. Sci.* **2012**, *417*, 174–182.
- [12] S. B. Adler, *Chem. Rev.* **2004**, *104*, 4791–4843.